Dalton Transactions

Accepted Manuscript

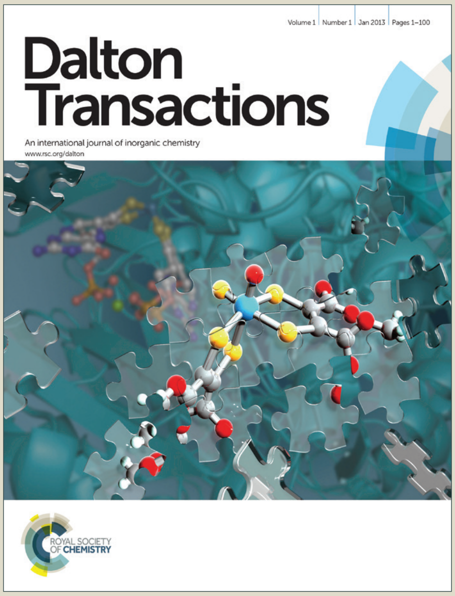

Volume 1 | Number 1 | Jan 2013 | Pages 1–100

Dalton Transactions

An international journal of inorganic chemistry

www.rsc.org/dalton

ROYAL SOCIETY OF CHEMISTRY

ROYAL SOCIETY OF CHEMISTRY

www.rsc.org/dalton

Cite this: DOI: 10.1039/c0xx00000x

www.rsc.org/xxxxxx

ARTICLE TYPE

Adsorption of Uranyl on Hydroxylated α-SiO_2(001): A First-Principle Study

Hui Wang,[a] Zhifang Chai,[a,b] Dongqi Wang*[a]

Received (in XXX, XXX) Xth XXXXXXXXX 20XX, Accepted Xth XXXXXXXXX 20XX

DOI: 10.1039/b000000x

The adsorption of $[UO_2(H_2O)_5]^{2+}$ on the hydroxylated α-SiO_2(001) surface was studied by periodic density functional theory (DFT) and ab initio molecular dynamics (AIMD) simulation. The effects of pH, CO_2, the aqua solution and anionic ligands (OH^-, NO_3^- and Cl^-) on the adsorption geometry and stability were investigated. The results show that the adsorption of uranyl on the hydroxylated α-SiO_2(001) surface leads to the formation of inner-sphere complexes, in which the bidentate complex at the double deprotonated site is most favored. The binding strengths of bidentate and monodentate complexes at the same site are similar, and become weaker as the number of protons increases at the adsorption site, indicating an enhancement of the adsorption strength at higher pH within a certain range. Strong chemical interaction plays an important role in all inner-sphere complexes. The hydrogen bonds are formed between uranyl and the hydroxylated surface in all inner- and outer-sphere complexes. The presence of CO_2 weakens the adsorption of uranyl on the surface by forming uranyl carbonate (CO_3^{2-}, HCO_3^-) complexes. The effect of the anion ligands depends on their charged state and their concentration in solutions. The explicit treatment of water environment in the models has slight effect on the adsorption configuration. These results are consistent with experimental observations.

Introduction

The migration of radionuclides in the natural environment has raised many concerns in nuclear technology and environmental chemistry for their threat to human's health and ecological environment.[1] Large amounts of radionuclides come from nuclear tests, spent nuclear fuel wastes and leakage at nuclear power stations.[2,3] After dissolved in groundwater, their precipitation and adsorption onto minerals is usually regarded as the second barrier and a key factor affecting the migration of radionuclides,[4] thus understanding the interaction between radionuclides and mineral surfaces is important for mastering their migration behavior in environment and the safety assessment of radioactive waste repositories.

Uranium is the most important nuclide because of its relatively high abundance in nature and the central role in the nuclear fuel cycle. The uranyl ion (UO_2^{2+}) is the dominant uranium species in contaminated groundwater systems due to its stability.[5] It is linear geometrically and has rich coordination chemistry with many ligands such as OH^-, CO_3^{2-}, NO_3^- and Cl^- in solutions. These uranyl species in solutions may be adsorbed on mineral surfaces, which is affected by many factors of the solution environment, such as the pH, the ionic strength and the presence of CO_2,[6-9] and has been studied by many groups with advanced experimental techniques such as EXAFS, TRLFS and batch experiments.[10-18] However, due to the complexity of these systems and the deficiency of experimental techniques, only limited information at the molecular level is available, and many experimental phenomena cannot be well explained.

Theoretical calculations offer new paths to study the actinide chemistry. [19-30] The First-principles method has proven to be a powerful tool and is successfully applied in the study of actinide adsorption on the mineral surfaces.[31-36] As a natural geologic material, silica is of great interest due to the abundance of silicate minerals in the environment, and its adsorption of uranyl has been studied experimentally.[6-8, 37-45] However, there are few theoretical works to address this subject up to now. It is thus highly desirable to characterize the adsorption of actinide on silica surface.

In the soil environment, the silica surface is known to be fully hydroxylated and surface silanol groups play a key role in sorption processes.[46] The pKa values of these surface functional groups were predicted to be in a wide range of 5.6-11.2 according to previous experimental and theoretical works.[47, 48] Herein the adsorption of $[UO_2(H_2O)_5]^{2+}$ from the aqua solution onto hydroxylated α-SiO_2(001) was studied by periodic DFT calculations and AIMD simulations in this work. Issues analyzed here cover the adsorption configurations, the effects of solvation, pH, CO_2 and anionic ligands (OH^-, NO_3^- and Cl^-) as well as the formation and binding energies. The Bader charge analysis[49-51] was also carried out to understand the charge transfer during the adsorption process and local density of states (LDOS) analysis was performed to understand the interaction between the uranyl and the surface.

Computational Details

All calculations were performed with the Vienna ab initio simulation package (VASP).[52, 53] The Perdew-Burke-Ernzerhof (PBE) functional[54] with the generalized gradient approximation (GGA) was used to describe the ion-electron interaction and the core electrons were described by the full-potential projector augmented wave (PAW) method[55, 56] with an energy cutoff of 500 eV for the plane-wave expansion. Scalar relativistic effects were incorporated into the effective core potentials via explicit mass-velocity and Darwin corrections. Geometry optimization was performed using the conjugate gradient algorithm until the forces on all unconstrained atoms were less than 0.02 eV/Å, and the spin polarization was considered for all calculations. Integrations in the Brillouin zone were performed using k-point grid generated with the Monkhorst–Pack grid, centered at the r-point. To evaluate the effect of van de Waals interaction on the adsorption and the kinetics of species on the metal surface, several key points were checked by an empirical dispersion correction using DFT-D3(BJ) method.[57,58]

The optimized primitive unit cell is characterized by the parameters a=b=5.01 Å, c=5.49 Å and $\alpha=\beta=90°$, $\gamma=120°$, agreeing well with the experimental values.[59] The derivation of the formation energy (ΔE_{form}) and the calculation of the binding energy (ΔE_{bind}) was according to Kremleva's[60] and Pan's work,[31] respectively. In order to allow long time AIMD simulations, the energy cutoff was reduced to 300 eV. The AIMD simulations with a time step of 1 fs were run with the NVT canonical ensemble, and the temperature was kept constant at 298.15 K using the Nose–Hoover thermostat.[61,62] The information about the model and details of computational method are given in the Supporting Information.

Results and Discussion

Uranyl adsorption on the hydroxylated α-SiO$_2$(001).

Both experimental and theoretical results show that $[UO_2(H_2O)_5]^{2+}$ is preferentially penta-coordinated in its equatorial plane.[63-66] The uranyl may interact with the hydroxylated α-SiO$_2$(001) surface via chemical bonding to form inner-sphere complexes or via hydrogen bonding in the outer-sphere complex (the optimized structure of uranyl and the surface are shown as Figure S1, in the Supporting Information). Both cases were investigated in this work. In inner-sphere complexes, uranyl may bind to one (monodentate) or two surface silanol O(OH) sites (bidentate) through U with the removal of one or two water ligands.

The two neighboring surface silanol O(H) sites with an O-O distance of 2.74 Å may be bonded to the same Si atom or two adjacent Si atoms (see Figure S1) and the surface site may be deprotonated (SiO) or remain protonated (SiOH) at different pH conditions. To address these distinct cases, six bidentate inner-sphere (SiOO, SiOOH, SiOHOH, SiO-SiO, SiO-SiOH and SiOH-SiOH), two monodentate (SiO and SiOH) and one outer-sphere complexes were investigated. For each complex, a few initial configurations were studied and the most stable ones were reported here with their configurations shown in Figure 1, and the key geometrical parameters, formation energies and binding energies collected in Table 1.

Inner-sphere: bidentate complex. *Two binding O(H) sites at the same Si atom.* When $[UO_2(H_2O)_5]^{2+}$ adsorbs on the surface to form a bidentate complex, two H_2O may be exchanged by two OH on the same Si atom, which are in the meantime dehydrogenated to facilitate the formation of a doubly deprotonated SiOO complex, as shown in Figure 1a. In this complex, $[UO_2(H_2O)_3]^{2+}$ locates at the SiOO bridge site with the O_{yl}-U-O_{yl} axis perpendicular to the plane of O_{surf}-Si-O_{surf}. The U atom binds to two deprotonated O_{surf} atoms with the U-O_{surf} distances of 2.27 and 2.29 Å, respectively, shorter than those to the aqua ligands (around 2.60 Å), indicating the stronger binding strength of U-O_{surf} than U-O_{wat}. The U-O_{surf} distances were determined to be 2.13 and 2.19 Å at AlOO site on the (001) surface of kaolinite,[67] and 2.21 and 2.23 Å at TiOO site on TiO_2(110).[31] The UO_2 group adapts itself to interact with the closest hydroxyl group via the hydrogen bond with an O_{yl}-H_{surf} distance of 1.98 Å. Hydrogen bonds are also formed between two H_2O molecules close to the surface and the surface silanol O_{surf} with the H_{wat}-O_{surf} distance of 1.70 and 1.84 Å, respectively. The distance of two silanol O_{surf} atoms at the adsorption site becomes shorter after uranyl adsorption (2.47 Å versus 2.74 Å). The U-Si distance representing the separation of uranyl and the surface is 2.97 Å, close to the experimental value of 3.1 Å obtained on the silica gel surface.[42]

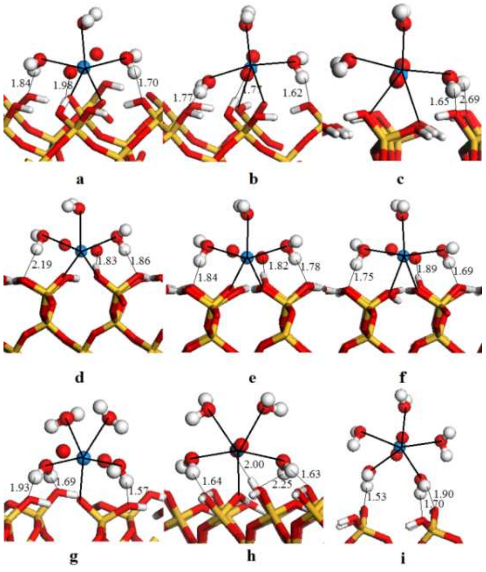

Figure 1 Optimized adsorption structures of uranyl adsorbed on the hydroxylated α-SiO2(001) surface. Inner-sphere: bidentate complex (a) SiOO (b) SiOOH (c) SiOHOH (d) SiO-SiO (e) SiO-SiOH (f) SiOHSiOH; monodentate complex (g) SiO (h) SiOH. Outer-sphere complex (i). Color scheme: U(blue), O(red), Si(orange), H (white).

A singly deprotonated SiOOH site may also present as an adsorption site for $[UO_2(H_2O)_3]^{2+}$ (see Figure 1b), which is closer to the deprotonated O_{surf} with a U-O_{surf} distance of 2.19 Å and farther from the protonated O_{surf}(H) (3.51 Å). The U-O_{wat} is longer than the U-O_{surf} and shorter than the U-O_{surf}(H). The O_{yl}-H_{surf} distance is 1.77 Å in this configuration and two H_{wat}-O_{surf} distances are 1.62 and 1.77 Å, respectively. The U-Si distance increases to 3.41 Å and the O_{surf}-O_{surf} distance of the adsorption site is 2.65 Å.

If the adsorption site does not deprotonate, the complex with

Table 1. Structure parameters (in Å), formation/binding energies (in eV) and the Bader charge (q_B in |e|) of surface in the inner-sphere and outer-sphere uranyl adsorption complexes on the hydroxylated α-SiO_2(001) surface. Q (in |e|) is the charge of the adsorption site.

Model	Q	U-O_{surf}	U-O_{yl}	U-O_{wat}	O_{yl}-H_{surf}	H-O_{surf}	$\Delta E_{form}/\Delta E_{bind}$	q_B
SiOO	-2	2.27,2.29	1.81,1.83	2.57,2.61,2.59	1.98	1.70,1.84	4.91(-7.63)	-1.29
SiOOH	-1	2.19,3.51	1.81,1.83	2.47, 2.49,2.56	1.77	1.62,1.77	1.13(-5.91)	-1.17
SiOHOH	0	2.53,2.70	1.81,1.82	2.48,2.56,2.61	-	1.65,2.69	-2.99(-3.74)	-0.97
SiO-SiO	-2	2.13,2.15	1.83,1.85	2.62,2.69,2.75	1.83	1.86,2.19	4.63(-8.69)	-1.21
		2.13,2.14	*1.83,1.85*	*2.61,2.68,2.77*	*1.80*	*1.82,2.21*	*4.30(-9.10)*	*-1.21*
SiO-SiOH	-1	2.14,2.49	1.82,1.84	2.61,2.61,2.61	1.82	1.78,1.84	-0.88(-5.93)	-1.14
SiOH-SiOH	0	2.53,2.64	1.82,1.84	2.55,2.56,2.57	1.89	1.69,1.75	-2.86(-4.01)	-0.94
SiO	-1	2.25	1.81,1.81	2.50,2.55, 2.62,2.64		1.57,1.69,1.93	1.19(-6.10)	-1.24
		2.24	*1.81,1.81*	*2.48,2.55,2.62,2.63*		*1.57,1.67,1.90*	*(-6.85)*	*-1.24*
SiOH	0	2.51	1.81,1.83	2.48,2.59,2.61,2.56		1.63,1.64,2.25	-2.37(-3.91)	-1.05
SiOHOH	0		1.82,1.82	2.50,2.52,2.57,2.63, 2.63		1.53,1.70,1.90	-1.05(-1.72)	-1.05
			1.81,1.82	*2.48,2.48,2.58,2.62,2.63*		*1.51,1.68,1.89*	*(-2.43)*	*-1.05*

The values in italic are obtained with the DFT-D3(BJ) method.

$[UO_2(H_2O)_3]^{2+}$ located at the SiOHOH site is formed, as shown in Figure 1c. The configuration is similar to that at the SiOO bridge site with U-O_{surf} distances of 2.53 and 2.70 Å, respectively, but the UO_2 group does not interact with the surface hydroxyl group via O_{yl} in this configuration. The distances of H_{wat}-O_{surf} are 1.65 and 2.69 Å. The U-Si distance is 3.37 Å and the O_{surf}-O_{surf} distance is 2.54 Å, which is the shortest in the SiOO complex.

In view of formation energy, the reactions leading to the formation of the former two complexes are endothermic by 4.91 and 1.13 eV, respectively, and that to the latter one is exothermic by 2.99 eV, suggesting the formation of the third complex (SiOHOH) is thermodynamically more favorable if starting from the protonated Si(OH)OH adsorption site on the surface, for the deprotonation of the surface is much endothermic. The binding energies are calculated to be -7.63, -5.91 and -3.74 eV, indicating strong interaction between the adsorbate and the surface which becomes weaker with the increase of surface H atoms at the adsorption sites. This can also be seen from the increased U-Si and U-O_{surf}(H) distances.

Using Bader's program, the Bader charge analysis was carried out to understand the fluctuation of electrostatic interaction during the adsorption process. The intact hydroxylated α-SiO_2(001) surface is -2 |e| charged while the uranyl moiety is +2 |e| charged before interaction. The Bader charge analysis shows that the surface remains negatively charged after adsorption, but the amount becomes smaller and the values for the three adsorption structures are -1.29, -1.17 and -0.97 |e|, respectively, indicating that the charge-charge interaction between the adsorbate and the surface is the strongest in the SiOO configuration and the weakest in the SiOHOH configuration. The charge transfer in the adsorption process weakens this electrostatic interaction.

Two binding O(H) sites at two adjacent Si atoms. $[UO_2(H_2O)_3]^{2+}$ can also bind with two surface silanol O(H) on two adjacent Si atoms, i.e., SiO(H)-SiO(H) site. The adsorption configurations are similar to that bound with two O atoms on the same Si atom and three cases were considered: the doubly deprotonated SiO-SiO (Figure 1d), the singly deprotonated SiO-SiOH (Figure 1e), and the doubly protonated SiOH-SiOH (Figure 1f).

In the SiO-SiO adsorption mode, the two U-O_{surf} and O_{yl}-H_{surf} distances are calculated to be 2.13, 2.15 and 1.83 Å, slightly shorter than that at the SiOO site, while the U-O_{yl}, U-O_{wat} and H-O_{surf} bonds are slightly longer. The shortest U-Si distance is 3.63 Å. The formation energy is also positive but smaller by 0.28 eV and the binding energy is larger by 1.26 eV, indicating stronger interaction. When it adsorbs at the SiO-SiOH site, the U-O_{surf} distances change to 2.14 and 2.49 Å, with the former one to the deprotonated SiO site and the latter to the protonated SiOH site, and other bonds U-O_{yl} (or O_{wat}), O_{yl}-H_{surf} and H-O_{surf} are slightly shorter than those at the SiO-SiO site. The shortest U-Si distance is 3.70 Å. The formation energy is -0.88 eV and the binding energy is -5.93 eV, smaller than that at the doubly deprotonated sites. When it adsorbs at the SiOH-SiOH site, the U-O_{surf} distances are 2.64 and 2.53 Å, respectively, longer than that at the deprotonated site. The shortest U-Si distance is 4.03 Å. The adsorption energy is calculated to be -2.86 eV and the binding energy is -4.01 eV.

Similar to the case at SiO(H)O(H) sites, Bader charge analysis was carried out, and the surface was found to remain negatively charged after adsorption with the values for the three adsorption structures being -1.21, -1.14 and -0.94 |e|, respectively, indicating that the charge-charge interaction is the strongest in the SiO-SiO configuration and the weakest in the SiOHOH configuration.

It is clear that both chemical binding and charge-charge interaction play important role in the adsorption process. To verify the strong chemical binding between the uranyl and the surface, the local density of states (LDOS) analysis was carried out for the bidentate complexes at the SiO(H)-SiO(H) sites and the orbital overlapping part below and nearest Fermi level were shown in Figure 2a-c. It is clear that both the U(d) and U(f) show strong hybridization with the O(p) at the SiO-SiO adsorption site (Figure 2a), indicating that strong chemical bonds are formed between them. At SiO-SiOH site, the O_{surf}(p) shows stronger

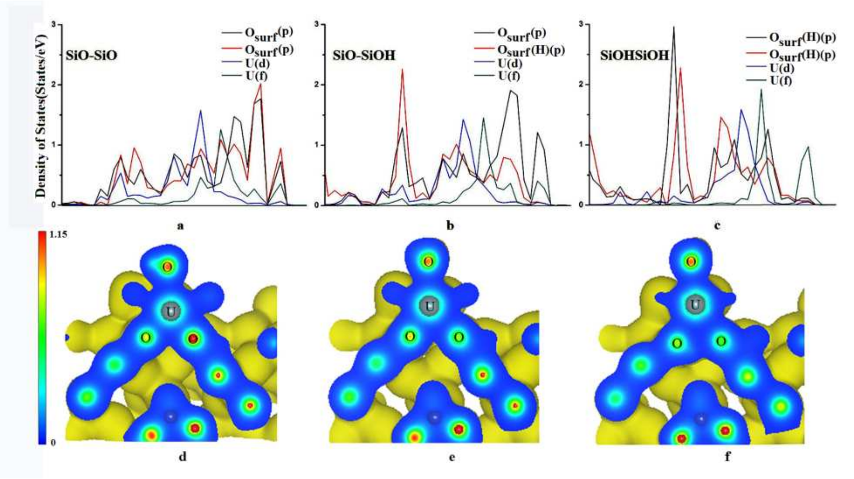

Figure 2 Local density of states (LDOS) and charge density of one orientation for uranyl adsorption at the SiO(H)-SiO(H) sites on the hydroxylated *α*-$SiO_2(001)$ surface. O(p) refers to the p-orbitals of two binding O atoms. Isosurfaces of charge density were calculated at 0.01 e Å^3.

hybridization with the U(f) than $O_{surf}(H)(p)$, while the hybridization is not obvious at the SiOH-SiOH site and the orbitals are relatively localized, indicating very weak chemical bonds. The electron density of one orientation plotted as Figure 2d-e give clear pictures. The vibrational frequency analysis for the adsorption complex at SiO-SiO site shows that the stretching mode of U-O_{surf} corresponds to 244 cm^{-1} and those of three U-O_{wat} bonds are 233, 221 and 214 cm^{-1}.

In summary, from the structure parameters of all bidentate complexes, we can see that uranyl binds to the surface O_{surf} through U which remains 5-fold coordinated in its equatorial plane in these configurations. In addition to the formation of U-O_{surf} coordination bond, uranyl also interacts with the surface through two H_2O ligands near the surface by forming hydrogen bonds. The much more charge the adsorbate and the surface carry at SiOO and SiO-SiO sites show the stronger charge-charge interaction than that at the singly and doubly protonated sites, with the latter even weaker, thus uranyl prefers to bind with the surface SiO site rather than the SiOH site, as also indicated by their stronger binding energy and the shorter distance of U-O_{surf} than U-$O_{surf}(H)$ as well as the U-Si distance. The negative binding energy indicates the strong binding interaction between the uranyl and the surface. Overall, both chemical binding and charge-charge interactions play important role in the adsorption process.

The binding interaction decreases as the number of protons at the adsorption sites implies that the adsorption of uranyl is weaker under acidic condition and the interaction is enhanced as pH increases in a certain range involving surface site deprotonation, while the pH dependence is minor under alkaline pH conditions since the surface deprotonation is complete and the surface site doesn't change anymore, in constant with the results in experiment.[6, 7, 38-40] Meanwhile, at high pH, the coordinating H_2O ligands may be replaced by OH^-, which may weaken the interaction between surface sites and uranyl species and will be discussed in latter section.

Note that, according to the formation energy, the deprotonation of the adsorption site needs more energy than released by the binding process for the formation of the complexes, indicating that under acidic and low temperature condition, it is highly possible to form the uranyl-silica complex with the adsorption sites protonated rather than deprotonated although uranyl prefers to bind with SiO than SiOH on the surface.

Inner-sphere: monodentate complex. When $[UO_2(H_2O)_5]^{2+}$ adsorbs on the surface forming monodentate complex, as shown Figure 1g-h, one coordinated H_2O is replaced by the $O_{surf}(H)$ at the adsorption site which may deprotonate or remain protonated during the adsorption process. In the former case, i.e. at the SiO site, the U-O_{surf} distance is calculated to be 2.25 Å, and both U-O_{yl} bonds are 1.81 Å. The four H_2O molecules are still in the first coordination shell with the U-O_{wat} distances around 2.60 Å. The hydrogen bonds are formed between two H_2O ligands closer to the surface and the surface O, with three H_{wat}-O_{surf} distances of 1.57, 1.69 and 1.93 Å. The adsorption configuration at the SiOH site is similar to that at the SiO site, with the U-O_{surf} distance slightly longer (2.51 Å). The shortest U-Si distance for the two configurations is 3.51 and 3.82 Å, respectively. The formation energy for the former one is endothermic by 1.19 eV, while exothermic by 2.37 eV for the latter one. The binding energies are -6.14 and -3.91 eV, respectively. The Bader charge analysis show that the surface was negatively charged after adsorption and the values for the two adsorption modes are -1.24 and -1.05 |e|, respectively.

Same conclusion can be obtained from the results for the monodentate complexes as that of the bidentate complexes: the attractive interaction is exist between uranyl and the surface; uranyl prefers to interact with SiO than SiOH group on the surface and the latter one is more favored in thermodynamics at acid condition; the charge-charge interaction between adsorbate and the surface is stronger in the complex at the SiO site than that at the SiOH site. However, the less exothermicity for the monodentate complex at the SiOH site than for the bidentate complex at the protonated sites (SiOHOH and SiOH-SiOH) indicates that the latter one is more favorable thermodynamically under the same pH condition.

All results of the inner-sphere complexes discussed above show that, under basic condition, the bidentate complex is more preferred concerning the much stronger binding energy for the SiO-SiO and SiOO complexes (-8.69 and -7.63 eV). The binding energies for the complexes at single deprotonated sites, i.e., SiO, SiO-SiOH and SiOOH are similar (-6.14, -5.93 and -5.09 eV), which is also the case for the complexes at the protonated sites, i.e., SiOH, SiOH-SiOH and SiOHOH (-3.91, -4.01 and -3.35 eV), indicating that the stability of the bidentate and monodentate adsorption complex of uranyl are similar under certain acidic condition where adsorption sites may present in the above-mentioned form and the binding strength become stronger as pH increases. The structure parameters, Bader charge and LDOS analyses also support these conclusions. In addition, both the adsorption on the deprotonated and protonated sites show strong chemical bonding and charge-charge interaction, suggesting that the adsorption process is not a simple ion-exchange process, in consistent with the experimental conclusion drawn based on the fact of the slow sorption rate of U(VI) on silica and the insensitivity to ionic strength of aqueous solutions.[7]

Outer-sphere complex. Uranyl can also adsorb on the surface via the H_2O ligands forming the outer-sphere complex. In this complex, the hydrogen bonds are formed between the two H_2O ligands near the surface and the surface O atoms with the H_{wat}-O_{surf} distances of 1.90, 1.70 and 1.53 Å. Both the two U-O_{yl} bonds are 1.82 Å long. The five H_2O ligands coordinated to U atom remain in the equatorial plane of uranyl with the U-O_{wat} distance of about 2.60 Å. The formation and binding energy of the outer-sphere complex are close, -1.05 eV versus -1.72 eV, implying that the deformation in the adsorption process is small. The much smaller binding energy than that of the inner-sphere complex indicates that the interaction between uranyl and the surface is much weaker in the outer-sphere complex, thus less preferred. Even though, the negative formation energy shows that the formation of outer-sphere complex is also feasible thermodynamically.

The Bader charge analysis shows that the surface was negatively charged after adsorption with a value of -1.05 |e|, smaller than the value of -2 |e| for the intact surface, indicating that the charge transfer between the adsorbate and the surface during adsorption weakens the charge-charge interaction between uranyl and the surface. In addition, the Bader charge is very close to that for the inner-sphere complexes, although the binding energy is much smaller for that only hydrogen bonding interaction is built in the outer-sphere complex, suggesting that the charge-charge interaction plays an equal role in all adsorption complexes at the same site, and the chemical bonding is important in the inner-sphere complexes.

In addition, we checked some representative case with the DFT-D3(BJ) method and the results are given in Table 1. It is found that the dispersion correction has slight effect of on the adsorption structures and Bader charge, while play important role on the forming and binding energies.

The effect of CO_2. Previous studies show that the adsorption of uranyl on mineral is sensitive to the atmospheric partial pressure of CO_2 (P_{CO2}) because of the formation of uranyl carbonate species under natural environment conditions.[37] As described in the Supporting Information, the $[UO_2(H_2O)(CO_3)]^0$ and $[UO_2(H_2O)(HCO_3)]^+$ complexes at the SiO(H)-SiOH sites were chosen as the model systems to study the influence of CO_2 on the adsorption of uranyl on hydroxylated α-SiO_2(001) and the optimized geometries are shown as Figure 3a-c.

The adsorption of $[UO_2(H_2O)(HCO_3)]^+$ at the SiOSiOH site (Figure 3a) shows strongest interaction among the three complexes. The U-O_{surf} bonds are 2.18 and 2.52 Å, and the O_{yl}-H_{surf} distance is 1.83 Å, similar to the adsorption $[UO_2(H_2O)_3]^{2+}$ at the same site, but slightly longer. The distances between U atom and the two binding O atom of HCO_3^- (2.48 and 2.45 Å) are much smaller than that with the O atom of the H_2O ligand (2.54 Å), indicating the much stronger binding between UO_2^{2+} and HCO_3^-. The order of distances U-O_{surf}<U-O_{carb}<U-O_{surf}(H) to some extent reflects the binding strength. Bader charge analysis shows that a charge transfer happens from the surface to the adsorbate, and the surface becomes less negatively charged with a value of -0.57 |e|, while the adsorbate less positively charged, which is much smaller than that for $[UO_2(H_2O)_3]^{2+}$ at the same site (-1.14 |e|). The binding energy is also much smaller, -4.93 eV versus -5.93 eV.

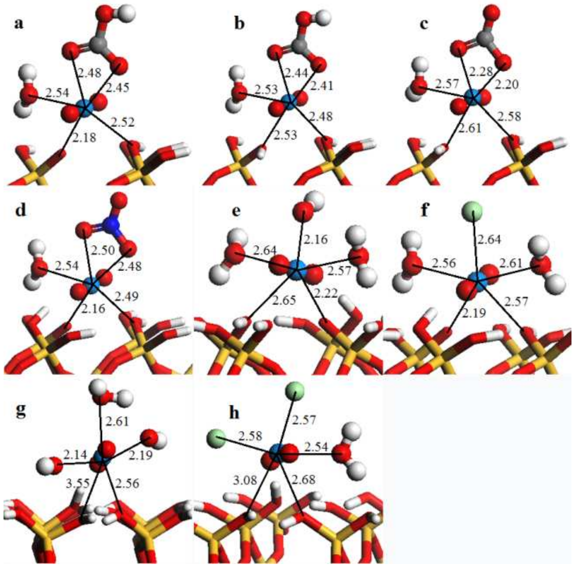

Figure 3 Optimized structure with key geometric parameters (in Å) of uranyl species adsorbed at the SiO(H)-SiOH sites of hydroxylated α-SiO_2(001). Color scheme: U(blue), O(red), Si(orange), H (white), C(grey), P(navy) Cl(green).

The adsorption configuration of $[UO_2(H_2O)(HCO_3)]^+$ at the SiOHSiOH site (Figure 3b) is similar to that at the SiOSiOH site with the longer U-O_{surf} and O_{yl}-H_{surf} distance of 2.53, 2.48 and 2.03 Å, indicating the weaker interaction. The U-O_{wat} distance and the distances between U atom and the two binding O atom of HCO_3^- is lightly shorter, 2.53, 2.44 and 2.41 Å, respectively, indicating the stronger interaction between uranyl and the ligands. The U-O_{carb} distance is also smaller than U-O_{surf}(H) in this configuration. Bader charge analysis shows that the surface is slightly negatively charged while the adsorbate is positively charged with a value of -0.46 |e|, which is much smaller than that for $[UO_2(H_2O)_3]^{2+}$ at the same site (-0.94 |e|). The binding energy is also much smaller, -3.11 eV versus -4.01 eV. The adsorption of $[UO_2(H_2O)(HCO_3)]^+$ at the SiOHSiOH site is smaller than that at the SiOHSiO site and the case is the same as that for $[UO_2(H_2O)_3]^{2+}$.

The adsorption of $[UO_2(H_2O)(CO_3)]^0$ at the SiOHSiOH site is in the similar configuration (Figure 3c), but the structure parameters are different. The U-O_{surf} bonds are 2.58 and 2.61 Å, much longer than those in other complexes at the same site. The U-O_{yl} bond and U-O_{wat} bond change slightly longer than $[UO_2(H_2O)(HCO_3)]^+$ at the same site and the distances between U atom and the two binding O atom of CO_3^{2-} become smaller and much shorter than that of U-O_{surf}(H), indicating the much stronger binding between UO_2^{2+} and CO_3^{2-}. Bader charge analysis shows that the surface is slightly positively charged while the adsorbate is negatively charged with a value of -0.10 |e|, which is much smaller than that for $[UO_2(H_2O)(HCO_3)]^+$ at the same site. The binding energy is also much smaller, -1.88 eV versus -3.11 eV. The binding strength at SiOHSiOH site follows the order: $[UO_2(H_2O)(CO_3)]^0 < [UO_2(H_2O)(HCO_3)]^+ < [UO_2(H_2O)_3]^{2+}$.

It is clear that, the Bader charge and binding energy for the adsorption of carbonate complex at the same site are much smaller than $[UO_2(H_2O)_3]^{2+}$, suggesting that the presence of CO_2 weakens the adsorption of uranyl on the surface of silica via the formation of carbonate complex which agrees with the experimental observations.[37] Thus, carbonate species are expected to play an important role in the migration behavior of radionuclides due to their high concentration in groundwater and their strong complexation ability towards uranyl. The negative effect on the adsorption may because the present of CO_3^{2-} (HCO_3^-) makes the uranyl species less positively (or neutral) charged, which is hard to adsorb on the less negatively (or neutral) charged sorbent surface. All the results show that the more positive charge on uranyl and the negative charge on the surface site, the stronger the interaction is, which can also be seen from Pan's results.[31]

Effect of other anionic ligands. The influence of other anionic ligands in addition to carbonate species on the adsorption of uranyl on minerals have also been studied experimentally.[41] Here, we focused on the effect of three types of most concerned anions, i.e. OH^-, NO_3^- and Cl^-, using the electro-neutral model mentioned above. The most preferential configurations are shown as Figure 3d-3f. The binding energy is calculated to be 4.99, -5.10 and 5.09 eV, respectively. The Bader charge analysis shows a charge transfer of -0.46 |e|, -.0.38 and -0.43 from the surface to the adsorbate in the three configurations, respectively. To investigate the effect of anion concentration on the adsorption, the complexes with two H_2O ligands replaced by two OH^- or Cl^- were studied and the most stable ones are shown as Figure 3g and 3h. The binding energy for the two configurations is 1.30 and 1.41 eV, respectively. The Bader charge transferred from the surface to the adsorbate is calculated to be 0.03 and 0.06 |e|, respectively.

In Figure 4, the calculated binding energies for all studied uranyl complexes are present. It is clear that, as the charge of the surface and/or adsorbate decreases, the E_{bind} value becomes smaller: the positively +2 charged complex $[UO_2(H_2O)_3]^{2+}$ at the negatively -2 charged doubly deprotonated site shows the strongest binding interaction, and the binding strength becomes weaker for the positive +1 charged adsorbates $[UO_2(H_2O)(HCO_3)]^+$, $[UO_2(H_2O)(NO_3)]^+$, $[UO_2(H_2O)_2(OH)]^+$, $[UO_2(H_2O)_2(Cl)]^+$ at the same singly deprotonated site which is negatively -1 charged. The neutral complexes $[UO_2(H_2O)(CO_3)]^0$, $[UO_2(H_2O)(OH)_2]^0$ and $[UO_2(H_2O)(Cl)_2]^0$ are found to bind to the neutral surface site most weakly. The charge of the surface changes with pH, while the charge of adsorbate is related to the charge of ligands. The more negative charge the ligands carry, the less positively charged the adsorbate, which leads to the weaker binding interaction. These results indicate that the charged nature plays important role in the adsorption process and the effect of different ligands depends on their charged state and concentration in solutions. This means that the influence of OH^- and carbonate species is important in groundwater, while the effect of other anions with much smaller concentration is negligible.

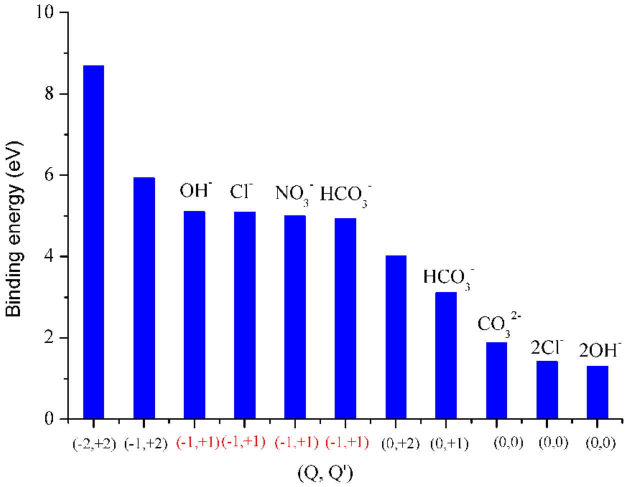

Figure 4 Calculated binding energies of uranyl species. The amount of charge of the surface site and adsorbate are denoted as Q and Q'.

Uranyl adsorption on the solvated α-SiO_2(001) surface.

Uranyl adsorption on the hydroxylated α-SiO_2(001) with an isolated water monolayer adsorption. To investigate how aqua solution may affect the adsorption of uranyl on the hydroxylated *α*-SiO_2(001) surface, we constructed models with an isolated water monolayer adsorbed on the surface according to Yang's[68] and Martorell's work[67] as described in the Supporting Information. The optimized configurations are shown in Figure S2 and the key geometric parameters are collected in Table S1.

It is found that uranyl remains penta-coordinated in its equatorial plane and the parameters are similar as that on the hydroxylated surface, while small difference is also observed due to the interaction with surrounding H_2O molecules. In the adsorption configuration of $[UO_2(H_2O)_3]^{2+}$ at the SiOHOH site, the O_{yl} atom does not form hydrogen bond with the surface SiOH group but with the solvent H_2O molecules around it instead. When it adsorbs at the SiOH-SiOH site, one water ligand turns around with one of its H atoms getting closer to U while the O atom moving farther. For other configurations, the U-O_{surf} distances become shorter and the U-O_{yl} bonds become longer, while the distances between U and aqua ligands change slightly. These similar results obtained with two models indicate that, the explicit treatment of water environment has slight effect on the adsorption configurations.

AIMD modeling of the adsorption uranyl on the hydroxylated α-SiO_2(001) in aqua solution. To evaluate the finite temperature effect and test the above models on the adsorption configuration of uranyl on the interface between hydroxylated *α*-SiO_2(001) and aqua solution, AIMD simulations were carried out at 298.15 K for the most favored configuration of uranyl adsorption at the SiO-SiO site.

It is found that the uranium on the water-silica interface remains penta-coordinated in its equatorial plane, similar to that at the SiO-SiO site on the hydroxylated α-SiO_2(001) surface without aqua solution. Different from the adsorption configuration on the hydroxylated α-SiO_2(001) surface with a water monolayer, the aqua solution around does not affect the orientations of water ligands of uranyl, indicating that the model without aqua solution employed here can reasonably mimic the adsorption of uranyl on the solvated hydroxylated silica surface in geometry, even better than the model with a water monolayer. The final structure of the equilibration run, i.e. the starting geometry of the production run, and the fluctuation of U-O_{surf} and U-O_{wat} distances during AIMD simulations are monitored and plotted in Figure 5. It is clear that the U-O_{surf} distances are around 2.2 Å and the U-O_{wat} distances are around 2.6 Å. Both of which are similar to the corresponding values without aqua solution, indicating that the DFT results obtained on the hydroxylated α-SiO_2(001) without aqua can reasonably reflect the behavior of uranyl on the water-silica interface.

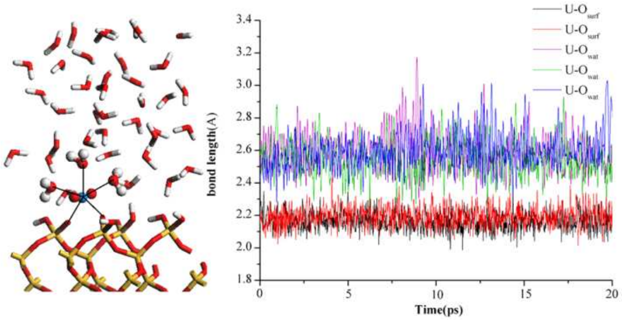

Figure 5 The adsorption configuration of uranyl on the hydroxylated α-SiO_2(001) surface with aqua solution (left) and key bond lengths as a function of simulation time during AIMD simulations.

Conclusion

In this work, the adsorption of $[UO_2(H_2O)_5]^{2+}$ on the hydroxylated α-SiO_2(001) surface and the effect of other anion ligands were studied by periodic DFT calculations, and the solution effect is modeled by adding a monolayer of water or a water box on the silica surface subject to geometrical optimization or AIMD. The results show that, the adsorption of uranyl prefers to form inner-sphere complexes. The binding interaction between the adsorbate and the surface is the strongest in the bidentate complex at the doubly deprotonated site and it is similar for the monodentate and bidentate complexes on the singly deprotonated site. The case is the same for the doubly protonated site, but the binding interaction becomes weaker as the increase of protons at the adsorption site. These results suggest that the adsorption of uranyl on the hydroxylated α-SiO_2(001) surface becomes stronger as pH increases in a certain range which facilitates the deprotonation of the surface site, and the pH dependence diminishes under alkaline pH conditions since the highly deprotonated surface site is no longer sensitive to the variation of basicity of the environment.

The adsorption process is not a simple ion-exchange or electrostatic adsorption process based on the fact that strong chemical interaction plays important role in all these inner-sphere complexes and the hydrogen bonds are also formed between the uranyl and the hydroxylated surface. The formation of outer-sphere complex by only building hydrogen bonds is also possible thermodynamically, but the binding interaction is much weaker. The Bader charge analysis shows that the charge-charge interaction between the uranyl and the surface is weakened by the charge transfer in the adsorption process and it is relatively stronger for the adsorption complex at the deprotonated site.

The presence of CO_2 weakens the adsorption of uranyl on the surface by forming uranyl carbonate and the complex with CO_3^{2-} is much weaker than that with HCO_3^- at the same adsorption site. The charged nature plays important roles in the adsorption process and the influence of the anion ligands such as OH^-, NO_3^- and Cl^- in addition to the carbonate ions depends on their charged state and their concentration in solutions. These results are consistent with the experimental observations. [6-8, 37-41]

When the uranyl adsorbs on the surface covered by a monolayer of water, the coordination mode and geometry parameters have little change, while the orientation of the water ligands changes slightly due to the interaction of water molecules around. The AIMD simulation employed the water-silica model at 295.15 K show that the aqua solution has little effect on the adsorption configuration which is the similar to the DFT results without aqua solution. These results indicate that handling of the aqua solution has slight effect on the adsorption configuration and the model systems without solution employed here can reasonably reflect the adsorption of uranyl on the interface of water-silica.

Acknowledgments

This work was financially supported by the National Natural Science Foundation of China to Z.Chai (91026000), to D.Wang (91226105), and by the Chinese Academy of Sciences to D.Wang (Y1515540U1, Y2291810S3), which are gratefully acknowledged. Calculations were done on the computational grids in the computer center of the Institute of High Energy Physics (IHEP), in the Supercomputing Center of Chinese Academy of Sciences (SCCAS) and in the National Supercomputing Center in Tianjin (NSCC-TJ).

Notes and references

[a] *CAS Key Laboratory of Nuclear Radiation and Nuclear Energy Techniques, and Multidisciplinary Initiative Center, Institute of High Energy Physics, Chinese Academy of Sciences, Beijing, 100049, China. E-mail: dwang@ihep.ac.cn*
[b] *School of Radiation Medicine and Interdisciplinary Sciences (RAD-X), Soochow University, Suzhou 215123, China*

† Electronic Supplementary Information (ESI) available: Detailed information on the computational method and configurations of uranyl adsorption on the hydroxylated α-SiO_2(001) surface with a water monolayer. See DOI: 10.1039/b000000x/

1 B. M. Thompson, P. A. Longmire, D. G. Brookings, *Appl. Geochem.* 1986, **1**, 335-343.
2 G. R. Choppin, *J. Radioanal. Nucl. Chem.* 2007, **273**, 695 -703.
3 D. L. Clark, D. E. Hobart, M. P. Neu, *Chem. Rev.* 1995, **95**, 25 -48.
4 H. Geckeis, J. Lutzenkirchen, R. Polly, T. Rabung, M. Schmidt, *Chem. Rev.* 2013**, 113** (2), 1016-1062.
5 I. Grenthe, R. J. M. Fuger, R. J. Konings, A. B. Lemire, A. B. Muller, C. Nguyen-Tsung Cregu, H. Wanner, Chemical thermodynamics of uranium, OECD Nuclear Energy Agency: North-Holland, 1992.
6 H. Zhang, C. Wen, Z. Tao, W. Wu, *J. Radioanal. Nucl. Chem.* 2011**, 287** (1), 13-20.
7 H. Zhang, Z. Tao, *J. Radioanal. Nucl. Chem.* 2002, **254** (1), 103-107.

8 E. S. Ilton, Z. Wang, J. F. Boily, O. Qafoku, K. M. Rosso, S. C. Smith, *Environ. Sci. Technol.* 2012, **46** (12), 6604-6611.

9 S. Kerisit, C. Liu, *Environ. Sci. Technol.* 2012, **46** (3), 1632-1640.

10 T. Reich, T. Y. Reich, S. Amayri, J. Drebert, N. L. Banik, R. A. Buda, J. V. Kratz, N. Trautmann, *AIP Conf. Proc.* 2007, **882**, 179-183.

11 C. J. Chisholm-Brause, J. M. Berg, K. M. Little, R. A. Matzner, D. E. Morris, *J. Colloid Interface Sci.* 2004, **277**, 366-382.

12 D. M. Singer, S. M. Chatman, E. S. Ilton, K. M. Rosso, J. F. Banfield, G. A. Waychunas, *Environ. Sci. Technol.* 2012**, 46**(7), 3811-3820.

13 P. C. Burns, K. M. Deely, S. Skanthakumar, *Radiochim. Acta* 2004, **92**, 151-160.

14 L. C. Shuller, R. C. Ewing, U. Becker, *Am. Mineral.* 2010, **95**, 1151-1160.

15 M. Harfouche, E. Wieland, R. Dähn, T. Fujita, J. Tits, D. Kunz, M. Tsukamoto, *J. Colloid Interface Sci.* 2006, **303**, 195-204.

16 J. Tits, G. Geipel, N. Mace, M. Eilzer, E. Wieland, *J. Colloid Interface Sci.* 2011, **359**, 248-256.

17 X. Tan, M. Fang, X. Wang, *Molecules* 2010, **15**(11), 8431-8468.

18 A. Křepelová, T. Reich, S. Sachs, J. Drebert, G. Bernhard, *J. Colloid Interface Sci.* 2008, **319**(1), 40-47.

19 Z. Szabó, T. Toraishi, V. Vallet, I. Grenthe, *Coord. Chem. Rev.* 2006, **250**, 784–815.

20 X. Tan, M. Fang, X. Wang. *Molecules* 2010, **15**, 8431-8468.

21 D. Wang, W. F. van Gunsteren, Z. Chai, *Chem. Soc. Rev.*, 2012, **41**, 5836–5865.

22 X.-D. Wen, R. L. Martin, T. M. Henderson, G. E. Scuseria, *Chem. Rev.* 2013, **113**, 1063−1096.

23 C. Walther, M. A. Denecke, *Chem. Rev.* 2013, **113**, 995−1015

24 A. Türler, V. Pershina. *Chem. Rev.* 2013, **113**, 1237−1312.

25 J. Qiu, P. C. Burns, *Chem. Rev.* 2013, **113**, 1097−1120.

26 P. J. Panak, A. Geist, *Chem. Rev.* 2013, **113**, 1199−1236

27 H. Nitsche, *Chem. Rev.* 2013, **113**, 855−857

28 K. E. Knope, L. Soderholm, *Chem. Rev.* 2013, **113**, 944−994.

29 M. Altmaier, X. Gaona, T. Fanghänel, *Chem. Rev.* 2013, **113**, 901−943.

30 D. Li, D. I. Kaplan. *J. Hazard. Mater.* 2012, **243**, 1–18.

31 Q. J. Pan, S. O. Odoh, A. M. Asaduzzaman,; G. Schreckenbach, *Chem. Eur. J.* 2012, **18** (5), 1458-1466.

32 J. Roques, E. Veilly, E. Simoni, *Int. J. Mol. Sci.* 2009, **10** (6), 2633-2661.

33 W. Yang, A. Zaoui, *Appl. Clay Sci.* 2013, **80-81**, 98-106.

34 D. M. Sherman, C. L. Peacock, C. G. Hubbard, *Geochim. Cosmochim. Ac.* 2008, **72** (2), 298-310.

35 X. Tan, X. Ren, J. Li, X. Wang, *RSC Advances* 2013**,** 3(42), 19551-19559.

36 L. V. Moskaleva, V. A. Nasluzov, N. Rösch, *Langmuir* 2006, **22**, 2141-2145.

37 J. D. Prikryl, A. Jain, D. R. Turner, R. T. Pabalan, *J. Contam. Hydrol.* 2001, **47**, 241–253.

38 J. N. Malin, J. G. Holland, S. A. Saslow, F. M. Geiger, *J. Phys.* Chem. C 2011, 115 (27), 13353-13360.

39 S. Nair, B. J. Merkel, *Geochem.* 2011, **17** (3), 209-219.

40 Y. Chi, Y. Chen, X. Liu, Z. Guo, L. Cai, *J. Radioanal. Nucl.Chem.* 2012, **292** (3), 1349-1355.

41 A. S. Kar, S. Kumar, B. S. Tomar, *Colloid Surf. A-Physicochem. Eng. Asp.* 2012, **395**, 240-247.

42 T. Reich, H. Moll, T. Arnold, M. A. Denecke, C. Hennig, G. Geipel, G. Bernhard, H. Nitsche, P. G. Allen, J. J. Bucher, N. M. Edelstein, , D. K. Shuh, *J. Electron. Spectrosc.* 1998, **96**, 237-243.

43 E. R. Sylwester, E. A. Hudson, P. G. Allen, *Geochim. Cosmochim. Ac.* 2000, **64**(14), 2431-2438.

44 T. Reich, H Moll, M. A. Denecke, G. Geipel, G. Bernhard, H. Nitsche, P. G. Allen, J. J. Bucher, N. Kaltsoyannis, N. M. Edelstein, D. K. Shuh, *Radiochmi. Acta*, 1996, **74**, 219-224.

45 Yu. D. Glinka, M. Jaroniec, V. M. Rozenbaum. *J. Colloid Inter. Sci.* 1997, **194**, 455-469.

46 D. Langmuir, Aqueous environmental geochemistry, 1st ed.; Pearson Education: Upper Saddle River, NJ, 1997.

47 D. Liu, G. Ma, H. C. Allen, *Environ. Sci. Technol.* 2005, **39**, 2025-2032.

48 M. Sulpizi, M.-P. Gaigeot, M. Sprik, *J. Chem. Theory Comput.* 2012, 8 (3), 1037-1047.

49 G. Henkelman, A. Arnaldsson, H. Jónsson, *Comput. Mater. Sci.* 2006, **36**, 254-360.

50 E. Sanville, S. D. Kenny, R. Smith, G. Henkelman, *J. Comp. Chem.* 2007, **28**, 899-908.

51 W. Tang, E. Sanville, G. Henkelman, *J. Phys.: Condens. Matter* 2009, **21**, 084204.

52 G. Kresse, J. Hafner, *Phys. Rev. B* 1993, **47**, 558–561.

53 G. Kresse, J. Furthermüller, *Phys. Rev. B* 1996, **54**, 11169–11186.

54 J. P. Perdew, K. Burke, M. Ernzerhof, *Phys. Rev. Lett.* 1996, 77, 3865-3868.

55 P. E. Blöchl, *Phys. Rev. B* 1994, **50**, 17953–17979.

56 G. Kresse, D. Joubert, *Phys. Rev. B* 1999, **59**, 1758–1775.

57 S. Grimme, J. Antony, S. Ehrlich, S. Krieg, *J. Chem. Phys.* 2010, **132**, 154104.

58 S. Grimme, S. Ehrlich, L. Goerigk, *J. Comp. Chem.* 2011**, 32,** 1456–1465**.**

59 L. Levien, C. T. Prewitt, D. J. Weidner, *Am. Mineral.* 1980, **65**, 920-930.

60 A. Kremleva, S. Krüger, N. Rösch, *Langmuir* 2008, **24**, 9515-9524.

61 S. Nosé, *J. Chem. Phys.* 1984, **81**, 511-519.

62 S. Nosé, *Prog. Theor. Phys. Suppl.* 1991, **103**, 1-46.

63 M. Åberg, D. Ferri, J. Glaser, I. Grenthe, *Inorg. Chem.*1983, **22**, 3986-3989.

64 M. da G. Miguel, S. J. Formosinho, A. C. Cardoso, H. D. Burrows, *J. Chem. Soc Faraday Trans.* 1984, 180, 1735-1744.

65 M. E. D. G. Azenha, H. D. Burrows, S. J. Formosinho, M. L. P. Leitão, M. da G. Miguel, *J. Chem.Soc. Dalton Trans,* 1988. 2893-2895.

66 P. G. Allen, J. J. Bucher, D.-K. Shuh, N. M. Edelstein, T. Reich, *Inorg. Chem.* 1997, 36 , 4676-4683.

67 B. Martorell, A. Kremleva, S. Krüger, N. Rösch, *J. Phys.* Chem. C 2010, 114, 13287–13294.

68 J. Yang, E. Wang, *Phys. Rev. B* 2006, **73** (3), 035406.

Table of contents entry

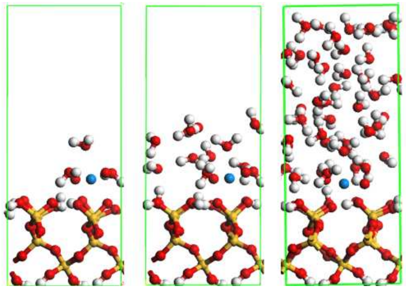

The effects of pH, CO_2, the aqua solution and anionic ligands on the adsorption of uranyl on α-SiO_2(001) were investigated.